J. Fluid Mech. (2007), *vol.* 583, *pp.* 123–132.
doi:10.1017/S0022112007006519 Printed in the United Kingdom

The motion of a prolate ellipsoid in a rotating Stokes flow

J. R. T. SEDDON AND T. MULLIN

Manchester Centre for Nonlinear Dynamics, University of Manchester
Oxford Road, Manchester, M13 9PL, UK

(Received 27 February 2007 and in revised form 26 April 2007)

Results are presented from experimental investigations into the motion of a heavy ellipsoid in a horizontal rotating cylinder, which has been completely filled with highly viscous fluid. The motion can be conveniently classified using the ratio between the maximum radius of curvature of the ellipsoid κ_{max} and the radius of the drum R_d. If $\kappa_{max} < R_d$ the ellipsoid adopts a fixed position adjacent to the rising wall for a given cylinder rotation rate. The dependence of this position on wall speed is, surprisingly, independent of the ellipsoid's length, and a Stokes flow model has been developed which predicts both this independence and the speed for the limiting case of an ellipsoid adjacent to a vertical wall. If $\kappa_{max} > R_d$ the ellipsoid must tilt in order to maintain the maximum surface area in close proximity to the wall. Once tilted, a component of the viscous drag acts to laterally translate the ellipsoid from end to end of the drum. The ellipsoid with $\kappa_{max} = R_d$ adopts a series of fixed positions for most drum rotational rates but, between two regions of fixed-point behaviour, it undergoes a transition to oscillatory motion.

1. Introduction

The motion of ellipsoidal particles in Stokes flows has been an interesting research topic for over a century. Oberbeck (1876) demonstrated that the viscous drag on an ellipsoid in an unbounded Stokes flow has a similar form to that for a sphere. The radius of the sphere is replaced by an *equivalent length scale* which is a geometric combination of the major and minor ellipsoid axes (Lamb 1932). Jeffery (1922) and Taylor (1923) presented theoretical and experimental results for the motion of an ellipsoid in a simple shear flow, whereas Wakiya (1957) studied the effects of distant boundaries to calculate the motion of an ellipsoid in a variety of geometries. Brenner & Gajdos (1981) investigated a sedimenting ellipsoidal particle very close to a wall and resolved the forces and torques on it as functions of both the ellipsoid's position and orientation.

The study of the motion of spheroidal particles in Stokes flows is important to help understand many biological systems. Oblate spheroids can be used to model platelets in blood flow (Mody & King 2005), whereas an ellipsoid with flagella or cilia is a good representation of bacteria, such as *Escherichia coli* (Bujalowski, Klonowska & Jezewska 1994), and an ellipsoid with no flagella or cilia can be used to model cyano-bacteria, such as *Synechococcus* (Albertano, Somma & Capucci 1997).

In the present study we investigate the motion of a heavy ellipsoid in a horizontal rotating drum, which has been fully filled with a very viscous fluid. We study the ellipsoid's motion at slow drum rotational rates, where it was found to lie adjacent to the rising drum wall, separated from the wall by a thin lubricating region, and located between the bottom (0°) and halfway up the cylinder wall (90°). A photograph

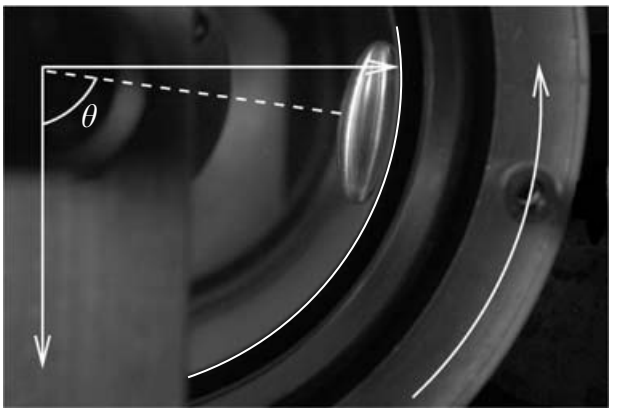

FIGURE 1. Photograph through the endcap of the rotating drum. The ellipsoid lies immediately adjacent to the rising drum wall, highlighted here by a white arc, at some azimuthal position θ. The arrows correspond to the vertical and horizontal axes and the direction of drum wall motion. The dashed line drawn to the midpoint of the ellipsoid is to demonstrate how the azimuthal position of the ellipsoid is measured.

of an ellipsoid at a fixed point, taken through an endcap of the drum, is shown in figure 1 where we also show the coordinate system. Our experimental studies show that the ellipsoid's motion falls into one of three categories, depending on the ratio between κ_{max}, the maximum radius of curvature of the ellipsoid, and the radius of the drum wall R_d (here $\kappa_{max} = a^2/b$, where a and b are the major and minor radii of the ellipsoid respectively). The qualitatively distinct types of motion are: (i) If $\kappa_{max} < R_d$ the ellipsoid sits at a series of fixed points against the wall, each corresponding to a different drum rotational rate. (ii) If $\kappa_{max} > R_d$ the ellipsoid is forced to tilt with respect to the direction of wall motion. A component of the viscous drag then acts to laterally translate the ellipsoid from end to end of the drum. (iii) If $\kappa_{max} = R_d$ the ellipsoid sits at a series of fixed points adjacent to the rising wall for a wide range of drum rotational rates, but then passes to a periodic regime where it oscillates in the direction of drum wall motion.

2. Method

The experiments were carried out using a horizontal glass drum of length 195 mm and inner radius $R_d = 60.00 \pm 0.02$ mm. The drum was levelled using an engineering spirit level and centred using ball races mounted in the endcaps. A DC feedback-controlled motor, connected via a gearbox and toothed-belt drive, was used to rotate the drum at a constant frequency and its rotational rate was monitored using an optical shaft encoder. This was found to be constant to within ± 0.001 Hz. The drum was fully filled with silicon oil with kinematic viscosity 1006 ± 10 cSt and housed in a temperature-controlled casing at $24.9 \pm 0.1\,^{\circ}$C. At this temperature, the shear viscosity and density of the oil were found to be 0.98 ± 0.01 Pa s and 974 ± 1 kg m^{-3} respectively by interpolating data from the fluid manufacturer. Dissolved gases in the fluid are known to alter the flow dynamics for different shaped particles (Yang *et al.* 2006; Seddon & Mullin 2006), so the oil was degassed using a vacuum pump over several hours.

Six ellipsoids were precision cut from an aluminium bar with density 2700 kg m^{-3} using a dedicated computer numerical control (CNC) machine. Each had the same minor radius of $b = 6.00 \pm 0.05$ mm and the major radii were $a = 7.00$, 10.00, 13.00,

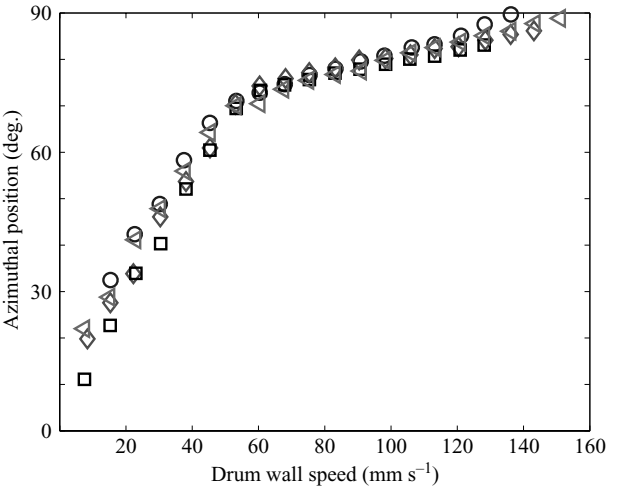

FIGURE 2. Azimuthal position of the ellipsoids with radius of curvature less than the drum, as a function of drum wall speed. The symbols correspond to ellipsoids with long axes of 7.00 (squares), 10.00 (triangles), 13.00 (diamonds) and 18.00 ± 0.05 mm (circles). The azimuthal position of the ellipsoids was independent of their long axes. Errors in the measured values are smaller than the symbols used to represent the data.

18.00, 19.00 and 22.00 ± 0.05 mm. The ellipsoids with $a \leqslant 18.00 \pm 0.05$ mm all satisfied $\kappa_{max} < R_d$, the ellipsoid with $a = 19.00 \pm 0.05$ mm had $\kappa_{max} = R_d$, and the $a = 22.00 \pm 0.05$ mm ellipsoid had $\kappa_{max} > R_d$.

Measurements of the azimuthal positions of the ellipsoids were taken using a protractor that was fixed in position in the stationary (laboratory) frame adjacent to an endcap of the drum. The dynamical motion observed for the $a = 19.00$ and 22.00 ± 0.05 mm ellipsoids was recorded using a 25 f.p.s. video camera, mounted horizontally and facing through the rising drum wall. Quantitative information on the period and amplitude of oscillation of the $a = 19.00 \pm 0.05$ mm ellipsoid, and for the translational speed and angular tilt of the $a = 22.00 \pm 0.05$ mm ellipsoid was obtained using image analysis tools on the individual frames of the movies.

3. Results and discussion

3.1. *Ellipsoids with* $\kappa_{max} < R_d$

The ellipsoids that satisfied $\kappa_{max} < R_d$ all aligned with their long axes parallel to the tangent of the wall at the position of closest approach, in the direction of wall motion, as in the example shown in figure 1. For a series of fixed drum rotational speeds, the ellipsoids were found to lie at a range of fixed azimuthal positions adjacent to the rising drum wall. Data for the azimuthal positions of the $a = 7.00$, 10.00, 13.00 and 18.00 ± 0.05 mm ellipsoids, as a function of the drum wall speed, are plotted in figure 2. All the ellipsoids behaved identically, i.e. for a fixed drum rotational rate they all aligned at the same azimuthal position adjacent to the rising drum wall and this dependence of position on drum wall speed was independent of the length of the ellipsoids' long axes. In general, the ellipsoid's were placed midway between the endcaps of the drum, although it is important to note that their motion was dominated by lubrication effects and hence the endwalls had no effect unless the ellipsoids were less than $\sim$12 mm from either end.

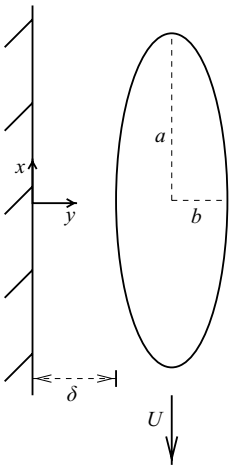

FIGURE 3. An ellipse with major and minor radii a and b lies adjacent to a vertical wall which rises at speed U. The wall and ellipse are separated by a thin lubricating region of minimum thickness δ. Note that the depth of the lubricating region has been greatly over-emphasized for clarity. In reality, δ is approximately four orders of magnitude smaller than a or b.

In order to understand this independence, we will consider the two-dimensional case of an ellipse adjacent to a rising vertical wall, as shown in figure 3. Implicit in this simplification is that the ratio of the gap thickness to the minor radius of an ellipsoid in the cross-stream direction is small. A thin band of lubrication is formed by flow between the wall and the length of the ellipsoid's surface. The strength of flow outside this region vanishes as $1/h^2$ (where h is defined in (3.2)) and so its contribution to the force on the ellipsoid is negligible. In the streamwise direction the lubrication approximation is valid over most of the ellipsoid's length because the minimum gap thickness δ is approximately 10^{-3} mm compared to a typical ellipsoid length scale of 10 mm. Using these simplifications, and the requisite that the pressure is only a function of the streamwise coordinate, the lubrication problem can now be solved from one end of the ellipse to the other.

An ellipse, with major and minor axes (a, b) respectively, lies adjacent to a rising wall which moves at speed U, separated by a thin lubricating region with minimum thickness δ, as shown in figure 3. The fluid flow in the lubricating region is governed by the Stokes equations (Batchelor 1967)

$$\mu \frac{\partial^2 u}{\partial y^2} = \frac{\partial p}{\partial x}, \tag{3.1}$$

where μ is the viscosity of the fluid travelling at speed u, and p is the pressure field within the gap. The coordinate system is Cartesian with origin on the wall, midway along the ellipse, and the surface of the ellipse is described by

$$h = b + \delta - b\left[1 - \left(\frac{x}{a}\right)^2\right]^{1/2}. \tag{3.2}$$

The flow is bounded by the no-slip conditions, such that $u = U$ on $y = 0$, and $u = 0$ on $y = h$. The speed of the fluid in the direction of wall motion is then

$$u = G\frac{y}{2\mu}[h - y] + U\left[1 - \frac{y}{h}\right], \tag{3.3}$$

where the pressure gradient $G = -\partial p/\partial x$. The volume flux is

$$Q = \int_0^h u \, \mathrm{d}y = \frac{Gh^3}{12\mu} + \frac{Uh}{2}, \tag{3.4}$$

and an expression for Q can be found by integrating the pressure derivative G obtained from (3.4) from end to end of the ellipse, where the pressures are both equal to p_0. This yields $Q = Uf_2/2f_3$, where $f_n = \int_{-a}^{a} h^{-n} \, \mathrm{d}x$.

The tangential force on the ellipse resulting from viscous drag is

$$F_{tang} = \mu \int_{-a}^{a} \left(\frac{\partial u}{\partial y} \right)_{y=h} \mathrm{d}x = \mu U \left(2f_1 - \frac{3f_2^2}{f_3} \right), \tag{3.5}$$

which balances its weight $\pi g \Delta\rho ab$, where $\Delta\rho$ is the density difference between the ellipse and the fluid.

The three functions f_1, f_2 and f_3 can be solved by using the substitution $\sin\theta = x/a$, such that

$$f_n = \int_{-\pi/2}^{\pi/2} \frac{a \cos\theta \, \mathrm{d}\theta}{(b + \delta - b\cos\theta)^n} \tag{3.6}$$

Evaluating (3.6) gives

$$f_1 = \frac{a}{b(\delta\Gamma)^{1/2}} \left[4(b+\delta) \arctan \left(\frac{\Gamma}{\delta} \right)^{1/2} - \pi(\delta\Gamma)^{1/2} \right], \tag{3.7}$$

$$f_2 = \frac{2a}{(\delta\Gamma)^{3/2}} \left[2b \arctan \left(\frac{\Gamma}{\delta} \right)^{1/2} + (\delta\Gamma)^{1/2} \right], \tag{3.8}$$

$$f_3 = \frac{a}{(\delta\Gamma)^{5/2}} \frac{1}{(b+\delta)} \left[6b(b+\delta)^2 \arctan \left(\frac{\Gamma}{\delta} \right)^{1/2} + (3b^2 + 4b\delta + 2\delta^2)(\delta\Gamma)^{1/2} \right], \tag{3.9}$$

where $\Gamma = (2b + \delta)$. After Goldman, Cox & Brenner (1967) we allow $\delta \to 0$ and in this limiting case, the $2f_1 - 3f_2^2/f_3$ term in the tangential force becomes

$$\lim_{\delta \to 0} \left(2f_1 - \frac{3f_2^2}{f_3} \right) = \frac{2a(2+\pi)}{b}. \tag{3.10}$$

Equating the viscous drag force with the ellipse's weight, the speed of the ellipse falling adjacent to a vertical wall is then

$$U = \frac{\pi g \Delta\rho b^2}{2\mu(2+\pi)}. \tag{3.11}$$

Several important observations can now be made: (i) the falling velocity of the ellipse is independent of its length because the three functions f_n are linearly dependent on a, thus balancing the linear dependence in the weight term. (ii) By inserting the experimental parameters for the ellipsoids used here into (3.11), the limiting speed of the ellipsoids at an azimuthal position of 90° against the drum wall can be predicted as $U_{pre} = 190\,\mathrm{mm\ s^{-1}}$, which is a satisfactory estimate for the experimentally found limit of $U_{exp} \approx 150\,\mathrm{mm\ s^{-1}}$. Note that we have ignored effects such as wall curvature and bulk flow in the drum and ellipsoid wake, and it is known from our work on spheres that these can have significant effects (Yang *et al.* 2006). In summary, the full three-dimensional problem is very difficult but our greatly simplified model contains the essence of the main result of length independence.

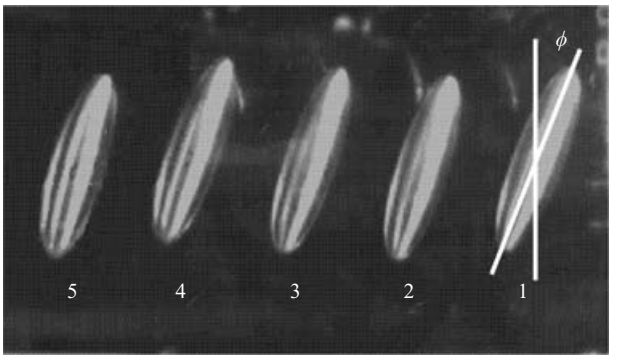

FIGURE 4. Time progression of the $a = 22.00 \pm 0.05$ mm ellipsoid as it translated laterally from the right- to the left-hand side of the drum. This image is a composition of five frames of a movie, recorded through the rising drum wall. The images are each separated by 15 s and the sequence runs from image 1 to 5. The angle of tilt of the ellipsoid is shown on image 1 as ϕ.

In order to predict the motion of an ellipsoid at azimuthal positions other than 90°, both the tangential and normal force balances need to be resolved. A similar problem arises for the case of a sphere moving adjacent to an inclined plane, as discussed by Ashmore, del Pino & Mullin (2005). They showed that cavitation breaks the symmetry of the flow field in the lubricating region and allows a normal force. Their lubrication model can be used to find an estimate for the size of a vapour cavity between an ellipsoid and wall. This should be approximately 0.5 mm, which is an order of magnitude larger than the resolution of the camera used to image the ellipsoid. However, no vapour cavity was observed for any of the ellipsoids and the normal force balance remains unresolved.

3.2. *Ellipsoids with* $\kappa_{max} > R_d$

An ellipsoid with $\kappa_{max} > R_d$ behaved strikingly differently to those with smaller curvature. The ellipsoid could not lie with its long axis parallel to the direction of wall motion and so tilted, as shown in figure 4. A component of the shear force acted to laterally translate the ellipsoid towards an end of the drum whereupon it systematically inverted its position about the axis tangent to the wall motion at the position of closest approach and translated back. A series of images representing the time progression of the ellipsoid's position is shown in figure 4. A similar lateral translation motion was also noted by Bluemink *et al.* (2005) who demonstrated that particle drift could be induced by particle asymmetry in a rotating flow.

Measurements of the azimuthal position and translational speed of the $a = 22.00 \pm 0.05$ mm ellipsoid, as a function of drum wall speed, are presented in figure 5. Both varied linearly with the drum wall speed for the measurable range of values. However, for azimuthal position angles smaller than ~20°, the ellipsoid moved in a stick–slip fashion, presumably because the thickness of the lubrication region was smaller than the characteristic roughness asperity size on the ellipsoid (~1.0 μm) and drum surfaces (~2.4 μm).

The angle of tilt of the ellipsoid's long axis with respect to the drum wall was constant at $\sim 35.8 \pm 0.2°$ for the entire range of drum wall speeds. This can be readily understood by a simple geometrical argument: if the ellipsoid is not tilted, its maximum radius of curvature in the (R_d, θ)-plane is 80.7 mm, whereas if the ellipsoid is tilted fully through 90°, i.e. with its long axis parallel to the drum axis, the maximum radius of curvature in the (R_d, θ)-plane is equal to the radius of the ellipsoid's small

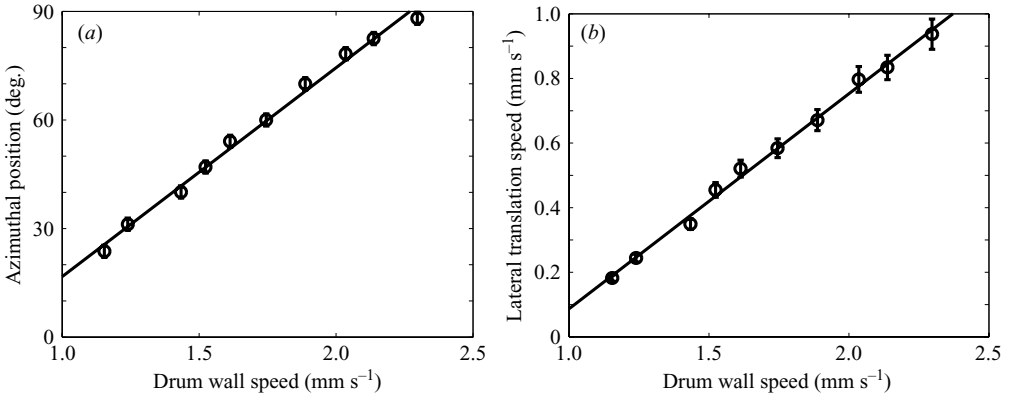

FIGURE 5. (*a*) Azimuthal position as a function of drum wall speed for the $a = 22.00 \pm 0.05$ mm ellipsoid. (*b*) The steady-state speed at which the ellipsoid translated from end to end of the drum, as a function of drum wall speed. The solid curves are linear fits to the data points. At angles lower than $\sim 20^{\circ}$, the thickness of the lubrication region was presumably smaller than the roughness level of the ellipsoid/drum and the ellipsoid moved in a stick–slip fashion.

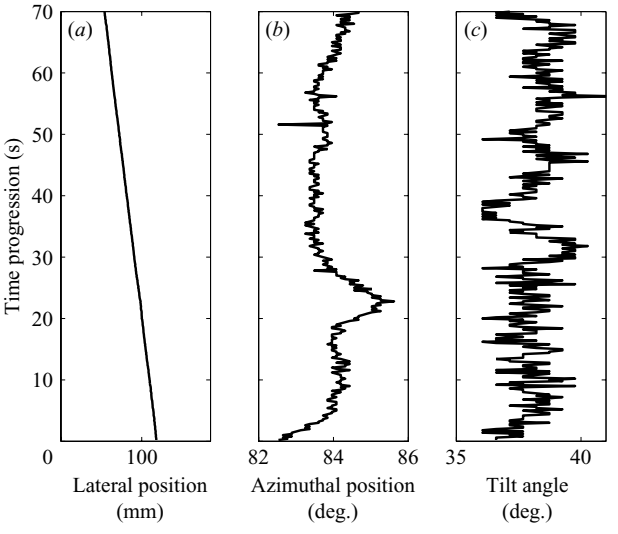

FIGURE 6. Time progression of the (*a*) lateral position, (*b*) azimuthal position, and (*c*) angle of tilt between long axis and direction of wall motion, for the $a = 22.00 \pm 0.05$ mm ellipsoid with a drum wall speed of 2.83 ± 0.03 mm s^{-1}. The ellipsoid translated smoothly from the right-hand end of the drum to the left, but its azimuthal position and angle of tilt both varied sporadically by $\pm 4^{\circ}$.

axis, 6.0 mm. This projected radius of curvature is equal to that of the drum wall when the ellipsoid has tilted through an angle of $\sim 36^{\circ}$ which is required for it to fit snugly against the wall.

It is important to note that the data presented in figure 5 have been averaged over an entire translation of the ellipsoid from one end of the drum to the other. For the specific case of a drum wall speed of 2.83 ± 0.03 mm s^{-1}, the time progression of the experimental parameters are plotted in figure 6, constructed by calculating instantaneous measurements of the various parameters for 70 s of the 25 f.p.s. video recording (1750 frames in total). The ellipsoid translated smoothly from end to end of

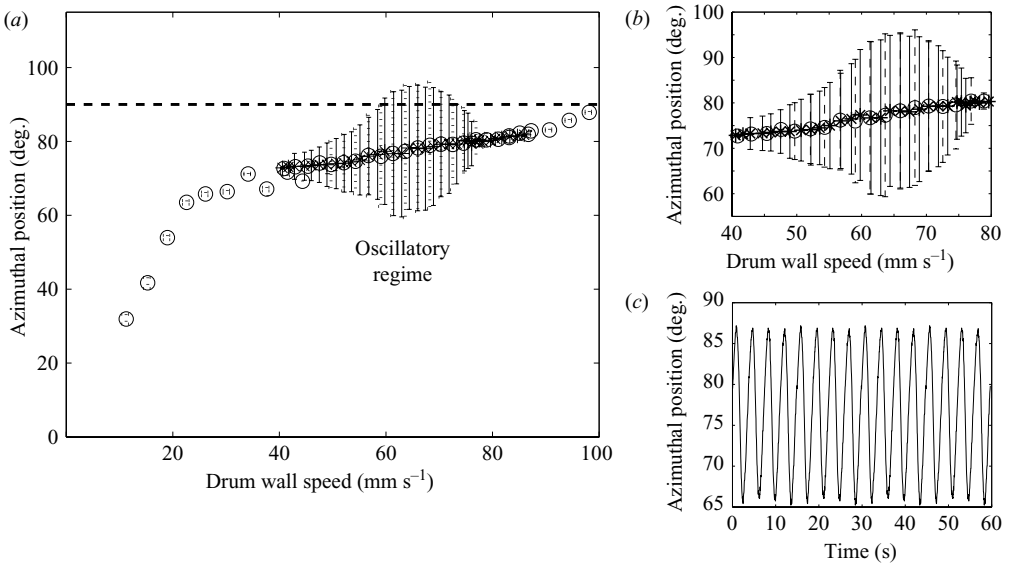

FIGURE 7. (*a*) Phase diagram for the $a = 19.00 \pm 0.05$ mm ellipsoid. Its motion was fixed-point for both very small and very large wall speeds but, for a large range of wall speeds ($\sim$40 to $\sim$80 mm s^{-1}) the ellipsoid passed from the fixed-point regime to an oscillatory one. Circles represent data taken with increasing drum speed, whereas stars represent data taken with decreasing drum speed. The error bars for data in the oscillatory regime correspond to the amplitude of oscillation and the horizontal dashed line represents an azimuthal position of 90°. To help distinguish between the increasing and decreasing data sets we have plotted the errorbars on the circles with dotted lines. (*b*) Detail of the oscillatory region. (*c*) Time sequence of azimuthal position at a drum speed of 55 mm s^{-1}.

the drum, but its azimuthal position and angle of tilt both varied sporadically about some fixed value (although within $\pm 4°$).

It is also important to note that no rotation of the ellipsoid was measured. One explanation of this is that the torque on the ellipsoid from fluid flowing in the lubrication region exactly balanced that from fluid in the outer flow field, as predicted for an infinitely long rod (Jeffery 1922). However, the tilt angle and position of the ellipsoid had significant variations, which gave rise to variations in the thickness of the lubrication region and, hence, in the relative strengths of the inner and outer torques. A more probable explanation is that the ellipsoid rotated extremely slowly. It is known that finite-length rods rotate with a surface speed of $\lesssim 1$ % that of the drum wall (Seddon & Mullin 2006) and we may expect ellipsoids to rotate slower than rods because only a fraction of the torque would be around the ellipsoid's long axis. Hence, it is likely that no rotation of the ellipsoid was detected because it reached the end of the drum before it had rotated by any measurable amount. The direction of rotation of the ellipsoid would be reversed when it reached the drum endcap and flipped, so no net rotation was measurable over several translations of the drum.

3.3. *Ellipsoid with* $\kappa_{max} = R_d$

An investigation into the special case of the ellipsoid with $\kappa_{max} = R_d$ was performed. This ellipsoid had length $a = 19.00 \pm 0.05$ mm. At slow drum rotational speeds the ellipsoid lay at a series of fixed positions adjacent to the rising drum wall, similar to the motion of the shorter ellipsoids. However, at a drum wall speed of $\sim$40 mm s^{-1} the ellipsoid began to oscillate up and down, adjacent to the wall, as indicated in figure 7.

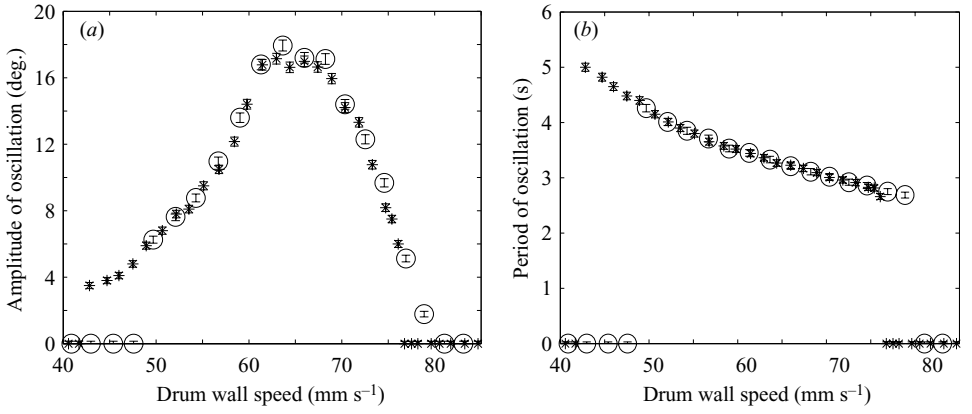

FIGURE 8. (*a*) Amplitude and (*b*) period of the oscillations, with hysteresis in both transitions between fixed-point behaviour and the periodic regime, for the $a = 19.00 \pm 0.05$ mm ellipsoid. Circles represent data taken with increasing drum speed, whereas stars represent data taken with decreasing drum speed.

This motion was periodic and robust with no observable variation in amplitude or period over extensive time periods (the maximum time observed was $\sim$4 days). At drum speeds $\gtrsim$80 mm s^{-1}, this periodic motion died away and the ellipsoid's motion became fixed-point once more. The error bars plotted for data in figure 7 in the oscillatory regime correspond to the amplitude of oscillation. Both the transitions between fixed-point and oscillatory motion were hysteretic. This can be seen more clearly in a graph of the amplitude of oscillation as a function of drum wall speed, plotted in figure 8(*a*). Surprisingly, during the oscillatory regime, the ellipsoid moved above the horizontal axis of the drum. The ellipsoid stayed adjacent to the wall and maintained a lubricating region between itself and the wall for the entire oscillatory cycle.

The period of oscillation as a function of drum wall speed is plotted in figure 8(*b*). With increasing drum wall speed the ellipsoid moved from fixed-point motion to the oscillatory regime with a sudden jump in the period of the oscillation, rather than growing slowly from zero. This period decreased with increasing drum wall speed until it suddenly returned to zero when the oscillations ceased. At a drum wall speed of $\sim$100 mm s^{-1}, the ellipsoid reached an azimuthal position of 90° in the fixed-point regime and fell from the wall, as expected.

4. Conclusions

We have investigated the motion of individual, heavy ellipsoidal particles in a horizontally rotating Stokes flow. The ellipsoids can exhibit three different types of motion, depending on their relative maximum radii of curvature with respect to that of the drum wall.

Ellipsoids with maximum radii of curvature smaller than the drum wall exhibit self-consistent behaviour. They align with their long axes parallel to the direction of drum wall motion and their motion is independent of their length. A simple Stokes flow model has been developed and agreement found with the experimental results.

We have previously shown that the motion of spheres and rods in a rotating drum is analogous to a particle translating and rotating down an inclined plane in a semi-infinite bath of fluid. However, the present results indicate that the behaviour of

ellipsoids is governed entirely by the geometry of the container. The role of cavitation in preventing contact between heavy rods and spheres and the wall is well-understood (Ashmore *et al.* 2005), but no cavitation was formed here and the source of the normal force between the ellipse and the wall remains unknown.

The ellipsoid with maximum radius of curvature equal to the drum wall exhibits fixed-point behaviour over a wide range of drum wall speeds. The oscillatory motion observed over the intervening range of speeds is curious in that the ellipsoid maintains its orientation with respect to the wall, rather than tumbling and moving in a more complicated fashion as may be expected (Yarin, Gottlieb & Roisman 1997).

The ellipsoid with maximum radius of curvature larger than the drum wall has to tilt in order to lie adjacent to the wall. The tilt is just sufficient to allow the point of closest approach between ellipsoid and wall to tend to zero. As the ellipsoid tilts, a component of the tangential force causes it to laterally translate from end to end of the drum. An intriguing aspect of the motion is that the translation of the ellipsoid is robust since its direction is catastrophically changed periodically when the particle reaches the endwall.

We gratefully acknowledge useful conversations with H. Brenner, A. M. J. Davis, J. Ashmore and M. Heil. J.S. is supported by a grant from the EPSRC and T.M. by an EPSRC Senior Fellowship.

REFERENCES

Albertano, P., Somma, D. Di & Capucci, E. 1997 Cyanobacterial picoplankton from the Central Baltic Sea: cell size classification by image-analyzed fluorescence microscopy. *J. Plankton Res.* **19**, 1405–1416.

Ashmore, J., del Pino, C. & Mullin, T. 2005 Cavitation in a lubricating flow between a moving sphere and a boundary. *Phys. Rev. Lett.* **94**, 124501.

Batchelor, G. K. 1967 *An Introduction to Fluid Dynamics*. Cambridge University Press.

Bluemink, J. J., van Nierop, E. A., Luther, S., Deen, N. G., Magnaudet, J., Prosperetti, A. & Lohse, S. 2005 Asymmetry-induced particle drift in a rotating flow. *Phys. Fluids* **17**, 072106.

Brenner, H. & Gajdos, L. J. 1981 London – van der waals forces and torques exerted on an ellipsoidal particle by a nearby semi-infinite slab. *Can. J. Chem.* **59**, 2004–2018.

Bujalowski, W., Klonowska, M. M. & Jezewska, M. J. 1994 Oligomeric structure of *Escherichia coli* primary replicative helicase DnaB protein. *J. Biol. Chem.* **269**, 31350–31358.

Goldman, A. J., Cox, R. G. & Brenner, H. 1967 Slow viscous motion of a sphere parallel to a plane wall-I Motion through a quiescent fluid. *Chem. Engng Sci.* **22**, 637–651.

Jeffery, G. B. 1922 The motion of ellipsoidal particles immersed in a viscous fluid. *Proc. R. Soc. Lond.* A **102**, 161–179.

Lamb, H. 1932 *Hydrodynamics*, 6th edn. Cambridge University Press.

Mody, N. A. & King, M. R. 2005 Three-dimensional simulations of a platelet-shaped spheroid near a wall in shear flow. *Phys. Fluids* **17**, 113302.

Oberbeck, A. 1876 Ueber stationäre flüssigkeitsbewegungen mit berücksichtigung der inneren reibung. *Crelles J.* **81**, 62–80.

Seddon, J. R. T. & Mullin, T. 2006 Reverse rotation of a cylinder near a wall. *Phys. Fluids* **18**, 041703.

Taylor, G. I. 1923 The motion of ellipsoidal particles in a viscous fluid. *Proc. R. Soc. Lond.* A **103**, 58–61.

Wakiya, S. 1957 Viscous flows past a spheroid. *J. Phys. Soc. Japan* **12**, 1130–1141.

Yang, L., Seddon, J. R. T., Mullin, T., del Pino, C. & Ashmore, J. 2006 The motion of a rough particle in a stokes flow adjacent to a boundary. *J. Fluid Mech.* **557**, 337–346.

Yarin, A. L., Gottlieb, O. & Roisman, I. V. 1997 Chaotic rotation of triaxial ellipsoids in simple shear flow. *J. Fluid Mech.* **340**, 83–100.